Modulation instability induced by cross-phase modulation with the fourth-order dispersion in dispersion-decreasing fiber

Taoping Hu (胡涛平)[1,2] and Xiaohan Sun (孙小菡)[1*]

[1] *National Research Center for Optical Sensing/Communications Integrated Networking, Lab of Photonics and Optical Communications, Department of Electronic Engineering, Southeast University, Nanjing 210096, China*

[2] *College of Science, Nanjing Forestry University, Nanjing 210037, China*

[*] *Corresponding author: xhsun@seu.edu.cn*

Received January 18, 2013; accepted April 12, 2013; posted online July, 2013

The modulation instability (MI) induced by cross-phase modulation (XPM) in dispersion-decreasing fiber (DDF), whose dispersion decreases along the direction of propagation, is solved and analyzed by the perturbation method for the extended nonlinear Schrödinger equation, considering the higher-order dispersion. The change of the gain spectra with incident power and dispersion decaying factor are also given respectively. Due to the fourth-order dispersion, XPM occurs at two gain spectral regions in both the normal and the anomalous dispersion regimes of DDF. The two gain spectral regions in the anomalous dispersion regime are larger than those in the normal dispersion regime. Moreover, the gain spectrum of the second region in the anomalous dispersion regime is near zero compared with that in the normal dispersion regime, indicating that XPM can be easily produced in the anomalous dispersion regime. The spectral width increases with the increase of the incident optical power and the dispersion decaying factor.

OCIS codes: 060.4370, 060.2330, 190.4370.

doi: 10.3788/COL201311.070602.

Nonlinear dispersion relation produces modulation instability (MI), i.e., the exponential growth of the amplitude of continuously weak perturbation caused by the interaction between dispersion and nonlinearity[1]. Cross-phase modulation (XPM), one main effect of nonlinearity, gives rise to a nonlinear phase modulation of each channel in a wavelength division multiplexing (WDM) system or an optical time division multiplexing (OTDM) system, depending on the overall power in all the other channels, with the power depending on the refractive index. XPM generates a great deal of interest because it can be used to realize all-optical demultiplexing, nonlinear pulse switching, wavelength converter, and tunable high repetition rate pulse trains[2−4]. Future ultrahigh bit-rate OTDM systems may require all-optical demultiplexing to down convert the high bit-rate data to where electronic circuits can be used. The most common device is the nonlinear optical loop mirror (NOLM), which allows switching due to XPM. As we know, NOLM relies on a nonlinear phase switch[3,4]. XPM also affects the waveform and spectrum of each optical signal during the transmission. By controlling the evolution of the signal spectrum, we can utilize this property of XPM to achieve efficient switching action for NOLM. Thus, it is very important to analyze the influence of XPM caused by higher-order dispersion to optical wave transmitting in NOLM. However, XPM also leads to pulse impairment and distortion, which seriously constrain the steady transmission of optical waves in fiber. Several theoretical and experimental studies measure the impact of XPM in WDM system[5−10]. There are also many theoretical studies about the nonlinear phase noise and crosstalk due to XPM[11−14]. Thus, the technologies to contain or suppress pulse impairments due to XPM using dispersion management and compensation attract considerable attention because XPM significantly degrades the quality of communication. One of them, for example, is XPM suppressor for multi-span dispersion managed WDM transmission[15,16]. Time domain phase conjugation (TDPC) and frequency domain phase conjugation (FDPC) are the other methods to improve the suppression and compensation due to the distortion caused by XPM[17].

However, the effect of XPM considering the higher-order dispersion has yet to be fully investigated. With the development of fiber communication, the emergence of large capacity, high bit-rate, high input optical power, and multi-channel in WDM and OTDM systems, the XPM effect due to the third- and fourth-order dispersions should be considered because this effect is inevitable and strong enough. It is reasonable to neglect the higher-order dispersion in common transmission because its influence is very little compared with that of group velocity dispersion (GVD). However, a previous experiment reports about the experimental observation of a new MI spectral window induced by the fourth-order dispersion in a normally dispersive single-mode optical fiber[18].

The recent research shows that XPM in dispersion-decreasing fiber (DDF), whose dispersion decreases along the direction of propagation, is more obvious than that in common standard single-mode fiber (SSMF); thus, DDF is a better dispersion medium to produce MI than the common SSMF[1]. In this letter, we study MI induced by XPM in DDF based on the extended nonlinear Schrödinger equation , while considering higher-order dispersion. The dispersion equation to describe XPM of higher-order dispersion is obtained theoretically. The characteristics of gain spectra in both the normal and the anomalous dispersion regimes of DDF are studied by simulation. These provide theoretical bases upon which

to discover ways to minimize the effect of XPM due to higher-order dispersion in WDM systems and to design new kinds of NOLMs.

Considering the effects of higher-order dispersion and fiber loss, the extended nonlinear Schrödinger equation describing any two optical waves transmitted in DDF can be written as[19]

$$\frac{\partial A_1}{\partial z}+\frac{1}{v_{g1}}\frac{\partial A_1}{\partial t}+\frac{\mathrm{i}}{2}\beta_{21}\frac{\partial^2 A_1}{\partial t^2}+\frac{\alpha_1}{2}A_1 = \frac{\beta_{31}}{6}\frac{\partial^3 A_1}{\partial t^3}-\frac{\mathrm{i}\beta_{41}}{24}\frac{\partial^4 A_1}{\partial t^4}+\mathrm{i}\gamma_1(|A_1|^2+2|A_2|^2)A_1, \quad (1)$$

$$\frac{\partial A_2}{\partial z}+\frac{1}{v_{g2}}\frac{\partial A_2}{\partial t}+\frac{\mathrm{i}}{2}\beta_{22}\frac{\partial^2 A_2}{\partial t^2}+\frac{\alpha_2}{2}A_2 = \frac{\beta_{32}}{6}\frac{\partial^3 A_2}{\partial t^3}-\frac{\mathrm{i}\beta_{42}}{24}\frac{\partial^4 A_2}{\partial t^4}+\mathrm{i}\gamma_2(|A_2|^2+2|A_1|^2)A_2, \quad (2)$$

where $A(z,t)$ is the amplitude of slow-varying envelop wave, t is time, z is transmission distance, v_{gj} is group velocity, and β_{kj} is the kth coefficient of the GVD of the jth optical wave. For common SSMF, β_{2j} is a constant, i.e., $\beta_{2j}(z)=\beta_{2j}(0)$, whereas $\beta_{2j}(z)=\beta_{2j}(0)\exp(-\mu_j z)$ for DDF. Where μ_j is the dispersion decaying factor of DDF, α_j is the coefficient of fiber loss, and γ_j is the nonlinear coefficient. In order to mathematically distinguish the two optical waves, we use subscripts 1 and 2 to describe them respectively. Suppose $A_1=u_1\exp(-\alpha_1 z/2)$ and $A_2=u_2\exp(-\alpha_2 z/2)$. Substituting them into Eqs. (1) and (2), we obtain

$$\frac{\partial u_1}{\partial z}+\frac{1}{v_{g1}}\frac{\partial u_1}{\partial t}+\frac{\mathrm{i}}{2}\beta_{21}\frac{\partial^2 u_1}{\partial t^2}=\frac{\beta_{31}}{6}\frac{\partial^3 u_1}{\partial t^3}-\frac{\mathrm{i}\beta_{41}}{24}\frac{\partial^4 u_1}{\partial t^4} +\mathrm{i}\gamma_1\left[u_1^2\exp(-\alpha_1 z)+2u_2^2\exp(-\alpha_2 z)\right]u_1, \quad (3)$$

$$\frac{\partial u_2}{\partial z}+\frac{1}{v_{g2}}\frac{\partial u_2}{\partial t}+\frac{\mathrm{i}}{2}\beta_{22}\frac{\partial^2 u_2}{\partial t^2}=\frac{\beta_{32}}{6}\frac{\partial^3 u_2}{\partial t^3}-\frac{\mathrm{i}\beta_{42}}{24}\frac{\partial^4 u_2}{\partial t^4} +\mathrm{i}\gamma_2\left[u_2^2\exp(-\alpha_2 z)+2u_1^2\exp(-\alpha_1 z)\right]u_2. \quad (4)$$

Under the condition of continuous and quasi-continuous waves, the amplitude u_j at $z=0$ is irrelative with time. The steady-state solutions of Eqs. (3) and (4) are given by

$$\bar{u}_1(z,t)=\sqrt{P_1}\exp\left\{\mathrm{i}\gamma_1\int_0^z[P_1\exp(-\alpha_1 z') +2P_2\exp(-\alpha_2 z')]\mathrm{d}z'\right\}, \quad (5)$$

$$\bar{u}_2(z,t)=\sqrt{P_2}\exp\left\{\mathrm{i}\gamma_2\int_0^z[P_2\exp(-\alpha_2 z') +2P_1\exp(-\alpha_1 z')]\mathrm{d}z'\right\}, \quad (6)$$

where P_1 and P_2 are the incident power at $z=0$. To study the stability of the steady-state solution, perturbing Eqs. (5) and (6) slightly, and suppose the perturbation items as $|a_1(z,t)|\ll P_1^{1/2}$ and $|a_2(z,t)|\ll P_2^{1/2}$, we have

$$u_1(z,t)=(\sqrt{P_1}+a_1)\exp\left\{\mathrm{i}\gamma_1\int_0^z[P_1\exp(-\alpha_1 z') +2P_2\exp(-\alpha_2 z')]\mathrm{d}z'\right\}, \quad (7)$$

$$u_2(z,t)=(\sqrt{P_2}+a_2)\exp\left\{\mathrm{i}\gamma_2\int_0^z[P_2\exp(-\alpha_2 z') +2P_1\exp(-\alpha_1 z')]\mathrm{d}z'\right\}. \quad (8)$$

Substituting Eqs. (7) and (8) into Eqs. (3) and (4), respectively, and linearizing a_1 and a_2, the perturbations a_1 and a_2 satisfy the following set of two coupled linear equations, and are expressed as

$$\frac{\partial a_1}{\partial z}+\frac{1}{v_{g1}}\frac{\partial a_1}{\partial t}+\frac{\mathrm{i}}{2}\beta_{21}\frac{\partial^2 a_1}{\partial t^2}=\frac{\beta_{31}}{6}\frac{\partial^3 a_1}{\partial t^3}-\frac{\mathrm{i}\beta_{41}}{24}\frac{\partial^4 a_1}{\partial t^4} +\mathrm{i}\gamma_1[P_1\exp(-\alpha_1 z)(a_1+a_1^*)+2(P_1P_2)^{1/2} \cdot\exp(-\alpha_2 z)(a_2+a_2^*)], \quad (9)$$

$$\frac{\partial a_2}{\partial z}+\frac{1}{v_{g2}}\frac{\partial a_2}{\partial t}+\frac{\mathrm{i}}{2}\beta_{22}\frac{\partial^2 a_2}{\partial t^2}=\frac{\beta_{32}}{6}\frac{\partial^3 a_2}{\partial t^3}-\frac{\mathrm{i}\beta_{42}}{24}\frac{\partial^4 a_2}{\partial t^4} +\mathrm{i}\gamma_2[P_2\exp(-\alpha_2 z)(a_2+a_2^*)+2(P_1P_2)^{1/2} \cdot\exp(-\alpha_1 z)(a_1+a_1^*)]. \quad (10)$$

Equations (9) and (10) can be solved by assuming a general solution of the form

$$a_j=U_j\cos(kz-\Omega T_j)+\mathrm{i}V_j\sin(kz-\Omega T_j), j=1,2, \quad (11)$$

where k is the wave number, Ω is the angular frequency of disturbance, and $T_j=t-z/v_{gj}$ (j=1,2) is delay time. Substituting Eq. (11) into Eqs. (9) and (10), allowing the real and imaginary parts of each equation be zero respectively, one can obtain a set of equations about U_1, V_1, U_2, and V_2. The sufficient and essential condition with nontrivial solution of this set is the determinant of the coefficient that should be zero, i.e.,

$$\left[\left(k-\frac{\beta_{31}}{6}\Omega^3\right)^2-f_1\right]\left[\left(k-\frac{\beta_{32}}{6}\Omega^3\right)^2-f_2\right]=C_{\mathrm{XPM}}, \quad (12)$$

where

$$f_j=\left(\frac{1}{2}\beta_{2j}\Omega^2-\frac{1}{24}\beta_{4j}\Omega^4\right) \cdot\left(\frac{1}{2}\beta_{2j}\Omega^2-\frac{1}{24}\beta_{4j}\Omega^4+2\gamma_j P_j\exp(-\alpha_j z)\right), j=1,2,$$

$$C_{\mathrm{XPM}}=16\gamma_1\gamma_2P_1P_2\exp[-(\alpha_1+\alpha_2)z] \cdot\left(\frac{1}{2}\beta_{21}\Omega^2-\frac{1}{24}\beta_{41}\Omega^4\right)\left(\frac{1}{2}\beta_{22}\Omega^2-\frac{1}{24}\beta_{42}\Omega^4\right).$$

Equation (12) becomes very complicated when fiber loss and higher-order dispersion are considered. For simplicity, suppose the third-order dispersions of two optical waves with little difference, i.e., $\beta_{31}\approx\beta_{32}=\beta_3$. The solution of Eq. (12) now becomes

$$\left(k-\frac{\beta_3}{6}\Omega^3\right)^2 =\frac{1}{2}\{(f_1+f_2)\pm\left[(f_1+f_2)^2+4(C_{\mathrm{XPM}}-f_1f_2)\right]^{1/2}\}. \quad (13)$$

In Eq. (13), when the sign "±" is minus and $C_{\rm XPM} > f_1 f_2$, we have $(k - \frac{\beta_3}{6}\Omega^3)^2 < 0$, and k is an imaginary number at this time. Then the disturbances a_1 and a_2 increase exponentially according to Eq. (11), which leads to MI phenomena when $C_{\rm XPM} > f_1 f_2$.

$$k = \frac{\beta_3}{6}\Omega^3 + \frac{\sqrt{2}}{2}\mathrm{i} \cdot \left\{\left[(f_1+f_2)^2 + 4(C_{\rm XPM} - f_1 f_2)\right]^{1/2} - (f_1+f_2)\right\}^{1/2}. \quad (14)$$

The definition of gain is[16] $g(\Omega) = 2\mathrm{Im}(k)$. From Eq. (14), we obtain

$$g(\Omega) = \sqrt{2}\{[(f_1+f_2)^2 + 4(C_{\rm XPM} - f_1 f_2)]^{1/2} - (f_1+f_2)\}^{1/2}. \quad (15)$$

In DDF, $\beta_2 = \beta_2(0)\exp(-\mu z)$. For simplicity, we suppose the difference between the two optical waves is very little, i.e., $\beta_{21}(0) \approx \beta_{22}(0) = \beta_2(0)$, $\gamma_1 \approx \gamma_2 = \gamma$, $\alpha_1 \approx \alpha_2 = \alpha$, $\mu_1 \approx \mu_2 = \mu$, and $\beta_{41} \approx \beta_{42} = \beta_4$. The condition of XPM $C_{\rm XPM} > f_1 f_2$ can be written as

$$16\gamma^2 p_1 p_2 \exp(-2\alpha z) > \left(\frac{\beta_2}{2}\Omega^2 - \frac{\beta_4}{24}\Omega^4 + 2\gamma p_1 \exp(-\alpha z)\right) \cdot \left(\frac{\beta_2}{2}\Omega^2 - \frac{\beta_4}{24}\Omega^4 + 2\gamma p_2 \exp(-\alpha z)\right). \quad (16)$$

Expanding it, we have

$$\Omega^8 - \frac{24\beta_2}{\beta_4}\Omega^6 - \left[\frac{48\gamma}{\beta_4}(P_1+P_2)\exp(-\alpha z) - \frac{144\beta_2^2}{\beta_4^2}\right]\Omega^4 + \frac{576\gamma\beta_2}{\beta_4^2}(P_1+P_2)\exp(-\alpha z)\Omega^2 - 6912\frac{\gamma^2 P_1 P_2}{\beta_4^2}\exp(-2\alpha z) < 0. \quad (17)$$

Equation (17) can be written as

$$(\Omega^2 - \Omega_1^2)(\Omega^2 - \Omega_2^2)(\Omega^2 - \Omega_3^2)(\Omega^2 - \Omega_4^2) < 0. \quad (18)$$

When Eq. (18) is satisfied, XPM can occur and the four parameters in Eq. (18) are

$$\Omega_{1,2,3,4}^2 = \frac{6\beta_2(0)\exp(-\mu z)}{\beta_4} \pm \frac{1}{\beta_4}\{36\beta_2^2(0)\exp(-2\mu z) + 24\gamma\beta_4(P_1+P_2)\exp(-\alpha z) \pm 24\gamma\beta_4\exp(-\alpha z)[(P_1+P_2)^2 + 12P_1P_2]^{1/2}\}^{1/2}, \quad (19)$$

when the former and later sign "±" being pluses corresponds Ω_1^2, former plus later minus Ω_2^2, former minus later plus Ω_3^2, and both minuses Ω_4^2.

In the anomalous dispersion regime of DDF, $\beta_2 < 0$ and $\beta_4 < 0$. Thus, $\Omega_2^2 < 0$ and $\Omega_4^2 > 0$. To get $\Omega_1^2 > 0$, from Eq. (18) we should have

$$3\beta_2^2(0)\exp(-2\mu z) - 2\gamma|\beta_4|\exp(-\alpha z)\{(P_1+P_2) + [(P_1+P_2)^2 + 12P_1P_2]^{1/2}\} > 0. \quad (20)$$

Now we obtain $\Omega_3^2 > 0$ and $\Omega_4^2 > \Omega_3^2 > \Omega_1^2 > 0$. Thus, Eq. (18) is satisfied when Ω is $0 < |\Omega| < |\Omega_1|$ or $|\Omega_3| < |\Omega| < |\Omega_4|$. This means that XPM can occur in two spectral regions, and that the fourth-order dispersion leads to a new spectral region of XPM in the anomalous dispersion regime.

In the normal dispersion regime of DDF, $\beta_2 > 0$ and $\beta_4 > 0$. Thus, $\Omega_1^2 > 0$ and $\Omega_3^2 < 0$. To obtain $\Omega_2^2 > 0$ and $\Omega_4^2 > 0$, we should have

$$3\beta_2^2(0)\exp(-2\mu z) + 2\gamma\beta_4\exp(-\alpha z)\{(P_1+P_2) - [(P_1+P_2)^2 + 12P_1P_2]^{1/2}\} > 0. \quad (21)$$

Under this condition, one can obtain $\Omega_1^2 > \Omega_2^2 > \Omega_4^2 > 0$. XPM occurs in two regions, namely, $0 < |\Omega| < |\Omega_4|$ and $|\Omega_2| < |\Omega| < |\Omega_1|$, indicating that in normal dispersion, the fourth-order dispersion also makes XPM appear in two spectral regions. From Eq. (19) we know that the fiber loss decreases the width of the spectral region.

XPM in DDF occurs in two spectral regions in the normal and anomalous regimes. Suppose the spectral region closer to zero is called the first spectral region and the one that is far from zero is called the second spectral region. The following figures can explicitly illustrate the conclusion by numerical simulation using Matlab. The parameters are $\beta_2 = \pm 20$ ps^2/km, $\beta_4 = \pm 0.02$ ps^4/km (the normal and anomalous dispersion regimes correspond to plus and minus, respectively), $\gamma = 2\,\mathrm{W^{-1}km^{-1}}$, $\alpha = 0.2$ dB/km, $\mu = 0.2$ dB/km, $z = 10$ km, and $P_2 = 10$ W.

Figures 1 and 2 show the gains of the first and second spectral regions in the normal and anomalous dispersion regimes for different P_1/P_2, respectively. As can be seen, the second spectral region is the new spectral region of XPM caused by the fourth-order dispersion. We can also find that the gains in the two regions increase with the increase of P_1/P_2, i.e., XPM in DDF becomes more obvious with the larger incident power of the optical waves, because the peak gain increases linearly with

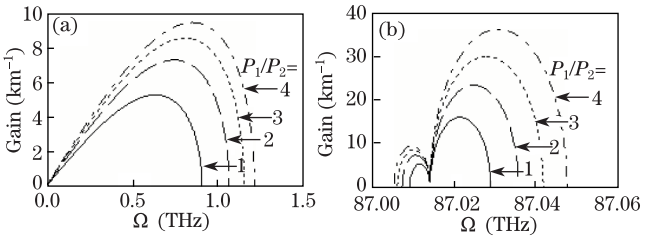

Fig. 1. Gain spectra of the (a) first and (b) second spectral regions in the normal dispersion regime.

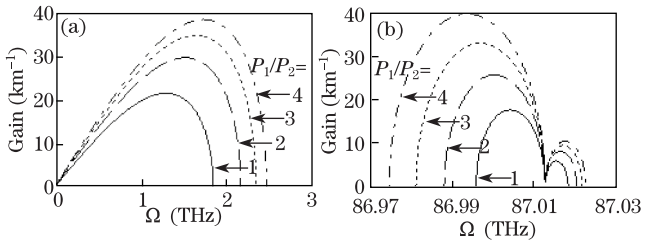

Fig. 2. Gain spectra of the (a) first and (b) second spectral regions in the anomalous dispersion regime.

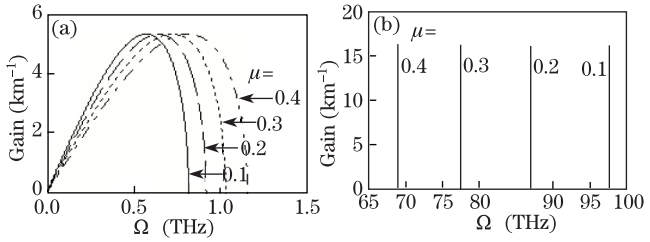

Fig. 3. Gain spectra of the (a) first and (b) second spectral regions in the normal dispersion regime for different values of μ.

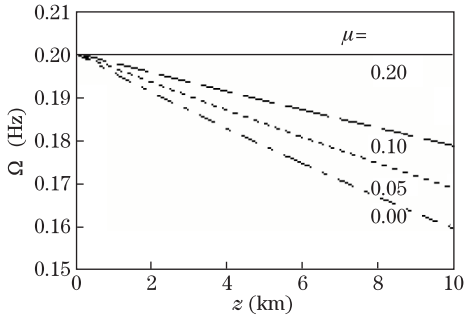

Fig. 4. Width of the first gain spectral region in the normal dispersion regime.

the incident power. The peak gain in the second spectral region is higher than that in the first spectral region; this physical phenomenon denotes that this MI of XPM can be expected to produce periodic trains of ultra-short pulses at higher repetition rates. Comparing Figs. 1 and 2, we find that the first and second spectral regions in the anomalous dispersion regime are wider than those in the normal dispersion regime, and the second spectral region in the anomalous dispersion regime is closer to the first spectral region than that in the normal dispersion regime. Although there are high and low peaks in both normal and anomalous dispersion regimes, the high peak in the anomalous dispersion regime is closer to the first spectral region than that in the normal dispersion regime. These indicate that XPM in DDF occurs more easily in the anomalous dispersion regime.

Figure 3 shows the gains of the first and second spectral regions in the normal dispersion regime for different values of μ. As can be seen, the first spectral region becomes wider with μ increasing for a certain transmission distance, and the second spectral region becomes closer to the first spectral region because of the increment of μ. However, the spectral regions are far from each other and the widths are small, it is difficult to directly compare them in Fig. 3. However, the numerical simulation shows the widths of the spectral regions are $\Delta\Omega_1 = 0.0651$ THz, $\Delta\Omega_2 = 0.0918$ THz, $\Delta\Omega_3 = 0.1297$ THz, and $\Delta\Omega_4 = 0.1830$ THz corresponding to values of μ that range from 0.1 to 0.4. It means that the second spectral region becomes wider and closer to the first spectral region with the increase of μ, and the same phenomenon occurs in the anomalous dispersion regime. These indicate that the dispersion decaying factor μ is beneficial to the production of MI induced by XPM in DDF.

Figure 4 shows the relation between the width of the first spectral region in the normal dispersion regime and the transmission distance z for different values of μ. From Fig. 4, we know that due to the effect of fiber loss, the spectral region becomes narrower with the increase of transmission distance. The main reason is that the intensity of the optical wave and the nonlinear effect become smaller with the increment of transmission distance due to fiber loss. However, the decreasing tendency becomes slower with the increase of μ, and when $\mu = 0.2\,\mathrm{dB/km}$, the width of the spectral region is almost unchangeable with variations in transmission distance z. This indicates that DDF is a better dispersion medium to produce XPM.

In conclusion, we study the MI induced by XPM in DDF based on extended nonlinear Schrödinger equation considering higher-order dispersion. Using this method, we obtain a general dispersion equation to describe XPM and numerically simulate it. The result shows that XPM in DDF occurs at two spectral regions in the normal and anomalous dispersion regimes due to the effect of the fourth-order dispersion. The spectral regions in the anomalous dispersion regime are wider than those in the normal dispersion regime, and the second spectral region in the anomalous dispersion regime is closer to the first spectral region than that in the normal dispersion regime, which indicates that XPM in DDF occurs more easily in the anomalous dispersion regime. The gain spectra become wider with the increase of P_1/P_2, i.e., the gain spectra become wider with larger incident power of the two optical waves. Furthermore, we find that the second spectral regions in the normal and anomalous regimes become wider and closer to the first spectral region with increasing values of μ. XPM in DDF also becomes increasingly obvious, which indicates that DDF is a better dispersion medium to create XPM. These findings provide theoretical bases upon which to discover ways to minimize the effect of XPM due to the higher-order dispersion in WDM systems and to design new kinds of NOLMs.

This work was supported by the National Natural Science Foundations of China under Grant Nos. 60972025 and 61271206.

References

1. S. M. Zhang, F. Y. Lu, W. C. Xu, and J. Wang, Opt. Fiber Technol. **11,** 193 (2005).
2. J. A. Bolger, P. F. Hu, J. T. Mok, J. L. Blows, and B. J. Eggleton, Opt. Commun. **249,** 431 (2005).
3. M. H. Yuan and L. Chen, Opt. Rev. **17,** 371 (2010).
4. J. Herrera, F. Ramos, and J. Marti, IEEE Photon. Technol. Lett. **17,** 2370 (2005).
5. J. D. Reis and A. L. Teixeira, Microw. Opt. Technol. Lett. **53,** 633 (2011).
6. H. B. Song and M. Brandt-Pearce, J. Lightwave Technol. **30,** 713 (2012).
7. M. Deng, X. Yi, J. Zhang, H. Zhang, and K. Qiu, Chin. Opt. Lett. **10,** 110602 (2012).
8. A. Argyris, E. Grivas, and A. Bogris, J. Lightwave Technol. **28,** 3107 (2010).
9. E. Tipsuwannakul, M. N. Chughtai, and M. Forzati, Opt. Express **18,** 24178 (2010).
10. M. Faisal and A. Maruta, Opt. Commun. **283,** 1899

(2010).

11. H. Kim, J. H. Lee,H. and C. Ji, Opt. Express **16,** 20687 (2008).
12. L. G. L. Wegener, M. L. Povinelli, A. G. Green, P. P. Mitra, J. B. Stark, and P. B. Littlewood, Phys. D **189,** 81 (2004).
13. Q. M. Nguyen and A. Peleg, Opt. Commun. **283,** 3500 (2010).
14. H. Zhou, K. Qiu, and F. Tian, Chin. Opt. Lett. **10,** 050601 (2012)
15. G. Bellotti and S. Bigo, IEEE Photon. Technol. Lett. **12,** 726 (2000).
16. X. Ma and C. Gan, Chin. Opt. Lett. **9,** 040602 (2011)
17. Y. Bu and X. Wang, Acta Phys. Sin. (in Chinese) **54,** 4747 (2005).
18. S. Pitois and G. Millot, Opt. Commun. **226,** 415 (2003).
19. G. P. Agrawal, *Nonlinear Fiber Optics* (Academic Press, San Diego, 2001).